Rescue of the Horseradish Peroxidase His-170 → Ala Mutant Activity by Imidazole: Importance of Proximal Ligand Tethering[†]

Sherri L. Newmyer,[‡] Jie Sun,[§] Thomas M. Loehr,[§] and Paul R. Ortiz de Montellano*[,‡]

Department of Pharmaceutical Chemistry, School of Pharmacy, University of California, San Francisco, California 94143-0446, and Department of Chemistry, Biochemistry, and Molecular Biology, Oregon Graduate Institute of Science and Technology, P.O. Box 91000, Portland, Oregon 97291-1000

Received April 17, 1996; Revised Manuscript Received July 16, 1996[⊗]

ABSTRACT: The proximal iron ligand in horseradish peroxidase (HRP) is His-170. The H170A mutant of polyhistidine-tagged HRP (hHRP) has been expressed in a baculovirus system and has been purified and characterized. At pH 7, the Soret maximum of the mutant is at 414 nm rather than 403 nm. Resonance Raman spectra indicate that the protein is primarily 6-coordinate low-spin in the ferric state with a band in the ferrous state at 212 cm^{-1} indicative of distal histidine coordination to the iron. Exogenous imidazole (Im) binds to the enzyme with $K_d = 22 \pm 4$ mM. Reaction of H170A hHRP with H_2O_2 does not give spectroscopically detectable compound I or compound II intermediates but results in gradual degradation of the heme group. Nevertheless, H170A hHRP is catalytically active, and its guaiacol and ABTS peroxidase activities are improved 260- and 125-fold, respectively, in the presence of saturating concentrations of Im. The K_m for the stimulatory effect of Im is 24 mM for both guaiacol and ABTS. The pH profile of H170A hHRP differs from that of wild-type hHRP, but the differences are essentially eliminated by Im. The rate of formation of "compound I" for H170A hHRP, determined by steady state kinetic methods, is $k_1 = 16\ M^{-1}\ s^{-1}$ without Im and $k_1 = 2.4 \times 10^4\ M^{-1}\ s^{-1}$ with Im. The corresponding rate for wild-type hHRP is $k_1 = 4.4 \times 10^6\ M^{-1}\ s^{-1}$. The results indicate that Im binds in the cavity created by the H170A mutation, coordinates to the heme iron atom, and restores a large part of the catalytic activity by rescuing the rate of compound I formation. However, this rescue of the catalytic activity by Im is possibly limited by coordination of the heme to the distal histidine (His-42) in the H170A mutant. Thus, a primary function of the proximal histidine is to tether the iron atom to disfavor sixth ligand binding, particularly coordination of the iron to the distal histidine. In addition, strong hydrogen bonding of the proximal ligand may be critical for facilitating O−O bond cleavage in the formation of compound I.

The fifth heme ligand is thought to play a key role in controlling the chemistry, and consequently the function, of the various classes of hemoproteins. The amino acid residues found as fifth ligands to the iron are histidine (e.g., globins, peroxidases), tyrosine (e.g., catalases), and cysteine (e.g., cytochromes P450, nitric oxide synthases). One important difference between these ligands is their electron-donating ability, because electron donation to the iron modulates its redox potential (Moore & Williams, 1977; Moore *et al.*, 1986), facilitates reactions such as dioxygen bond cleavage at the distal (sixth) coordination site (Traylor & Popovitz-Biro, 1988; Dawson, 1988), and stabilizes hypervalent iron intermediates (Walker *et al.*, 1976; Doeff & Sweigert, 1982; Tondreau & Sweigert, 1984; Du & Loew, 1995). Thiolate is the most, and imidazole (Im)[1] the least, electron-donating ligand, although the electron-donating properties of a histidine can be enhanced by interactions that increase its imidazolate character. Indeed, the NMR shift of the histidine N-1 proton, which reflects the degree of imidazolate character of the ligand, is inversely but linearly related to the redox potential for metmyoglobin, lignin peroxidase, CCP, and HRP (Banci *et al.*, 1991). The crystal structure of CCP shows that the proximal histidine forms a hydrogen bond with an aspartate residue (Asp-235) (Finzel et al., 1984). Partial deprotonation of the proximal histidine appears to be a characteristic of the peroxidases because the histidine is hydrogen bonded to an aspartate or asparagine not only in CCP but also in all the peroxidases for which crystal structures are available, including ascorbate peroxidase (Patterson & Poulos, 1995), lignin peroxidase (Poulos et al., 1993), *Arthromyces rhamosus* peroxidase (Kunishima et al., 1994), and myeloperoxidase (Zeng & Fenna, 1992).

The role of the proximal histidine ligand in peroxidase function has been most extensively studied for CCP. Replacement of the proximal CCP ligand (His-175) by a glutamine or glutamate yields enzymes with k_{cat} values for cytochrome *c* and ferrocyanide peroxidation comparable to those for wild-type CCP (Choudhury *et al.*, 1994). Resonance Raman and X-ray studies have confirmed that the iron in the H175E mutant is coordinated to an oxygen of the glutamic acid (Choudhury et al., 1994; Smulevich et al.,

[†] This work was supported by National Institutes of Health Grants GM32488 (P.R.O.M.) and GM34468 (T.M.L.).

* Author to whom correspondence should be addressed. FAX: (415) 502-4728 Email: ortiz@cgl.ucsf.edu.

[‡] University of California, San Francisco.

[§] Oregon Graduate Institute of Science and Technology.

[⊗] Abstract published in *Advance ACS Abstracts,* September 15, 1996.

[1] Abbreviations: HRP, native horseradish peroxidase isozyme *c*; hHRP, polyhistidine-tagged recombinant horseradish peroxidase isozyme *c*; CCP, cytochrome *c* peroxidase; heme, iron protoporphyrin IX regardless of oxidation and ligation state; BSA, bovine serum albumin; Im, imidazole; ABTS, 2,2′-azinobis(3-ethylbenzothiazoline-6-sulfonic acid); rRaman, resonance Raman.

S0006-2960(96)00933-6 CCC: $12.00

1995). Replacement of the proximal histidine by a cysteine gives a much less active protein, but crystallographic studies show that the cysteine has been oxidized to cysteic acid and is coordinated to the iron through an oxygen atom. Mutation of the proximal histidine to a glycine yields an enzyme in which the iron is coordinated to two water molecules (McRee *et al.*, 1994). This bisaquo H175G enzyme retains only 1.6% of the wild-type activity, but its activity increases ~3-fold in the presence of a saturating concentration of exogenous Im. Crystallographic studies show that the exogenous Im binds in the cavity created by the H175G mutation and coordinates to the iron, but the turnover data indicate that it is a relatively poor substitute for the normal histidine ligand (McRee *et al.*, 1994). These studies suggest that catalytic turnover is modestly enhanced by proximal ligands other than water but is relatively insensitive to the exact nature of the ligand. However, this inference appears to conflict with the results of mutating Asp-235 to a glutamine or glutamic acid. A D235N mutation, which eliminates the hydrogen bond between Asp-235 and His-175, markedly decreases (>1000-fold) the peroxidase activity of CCP (Goodin & McRee, 1993). In contrast, a D235E mutation, in which a hydrogen bond is preserved, gives a protein with 41% of the wild-type activity. The discrepancy between the sensitivity of enzyme activity to the presence of the His−Asp hydrogen bond and the evidence that the nature of the proximal ligand is not critical suggests that the role of the hydrogen bond in tethering or positioning the histidine ligand may be as important as its role in increasing the imidazolate character of the ligand.

The following sequential reactions are catalyzed by HRP, CCP, and other peroxidases:

$$\text{HRP} + \text{H}_2\text{O}_2 \xrightarrow{k_1} \text{compound I} \quad (1)$$

$$\text{compound I} + \text{AH} \xrightarrow{k_2} \text{compound II} + \text{A}\cdot \quad (2)$$

$$\text{compound II} + \text{AH} \xrightarrow{k_3} \text{HRP} + \text{A}\cdot \quad (3)$$

The first reaction is a two-electron oxidation of the protein to give compound I, which consists of a ferryl (Fe^{IV}=O) species and either a porphyrin (HRP) or a protein (CCP) radical cation (e.g., Ortiz de Montellano, 1992). In the second step, transfer of an electron from a substrate (AH) such as guaiacol or ABTS quenches the porphyrin or protein radical and produces compound II, which retains the ferryl species. A second electron transfer from a substrate molecule regenerates the resting ferric enzyme.

Little information is available on the function of the proximal ligand in HRP and related peroxidases despite the fact that its role, as suggested by the differences in compound I structures, may differ from that in CCP. A new approach to examination of the role of the metal ligand in hemoproteins involves site-specific replacement of the coordinating residue by a noncoordinating amino acid. The cavity thus created makes possible the coordination of exogenous ligands to the metal. This technique was first applied to ligand replacement in non-heme proteins (Berg et al., 1991; den Blauuwen & Canters, 1993), but in the hemoprotein field was first applied to myoglobin (Barrick, 1994, 1995; DePillis *et al.*, 1994). As discussed earlier, ligand replacement by this method has been investigated with CCP (McRee *et al.*, 1994). We report here the preparation and characterization of H170A hHRP, a mutant enzyme in which the proximal histidine ligand has been replaced by an alanine, and partial rescue of the catalytic activity of the mutant by exogenous Im.

EXPERIMENTAL PROCEDURES

Materials and Methods. Recombinant, polyhistidine-tagged hHRP (denoted as "wild-type") was expressed in *Escherichia coli* and was purified as previously reported (Newmyer & Ortiz de Montellano, 1995). Native HRP was from Boehringer Mannheim and BSA-bound Sepharose from Bio-Rad. Kinetic assays and spectra were carried out on a Cary 1E or a Hewlett Packard 8452A diode array spectrophotometer. H170A hHRP was quantitated by the Bradford assay (Bio-Rad), using BSA as a standard. Heme content was determined by the pyridine hemochromogen assay (Furhop & Smith, 1975).

Expression and Purification of the H170A hHRP Mutant. The protocol for expression and purification of the H170A mutant was similar to that used to obtain the H42A, H42V, and F41A hHRP mutants (Newmyer & Ortiz de Montellano, 1995). Cassette mutagenesis, performed on pUC-HRP (British Biotechnologies), was carried out using a cassette flanked by *Bsp*M II (*Bsp*E I) and *Bst*E II restriction sites and encoding an alanine at position 170 of the protein. Subcloning of the mutated HRP gene into a polyhistidine-tag-encoded version of the baculoviral vector pACGP67 was done as described earlier to allow for the expression of the protein with an N-terminal polyhistidine-tag (Newmyer & Ortiz de Montellano, 1995). Amplification of the baculoviral stock and production of H170A hHRP were done as described for H42A, H42V, and F41A hHRP. The affinity purification method used to isolate the earlier mutants was also used to purify the H170A hHRP mutant.

Assay of Guaiacol and ABTS Activities. Guaiacol and ABTS activities were monitored spectrophotometrically at 20 °C. In rescue experiments, H170A hHRP was preincubated with Im (0.5−50 mM) for 2 h at 20 °C prior to assay because the binding of Im is a slow process. To assay guaiacol activity, the Im-preincubated enzyme was diluted into assay buffer containing 5 mM guaiacol in 20 mM Na_2HPO_4, pH 6.0, giving a final enzyme concentration of 0.94 μM in a total volume of 1 mL. H_2O_2 (0.5 mM) was added to initiate the reaction, and guaiacol consumption was monitored at 470 nm (ϵ_{470} = 2.75 mM^{-1} cm^{-1}) (Newmyer & Ortiz de Montellano, 1995). ABTS activity was measured by diluting the same amount of enzyme into 1 mL of 20 mM NaOAc, pH 5.0, buffer containing 5 mM ABTS. H_2O_2 (0.5 mM) was added to initiate the reaction and formation of the ABTS radical cation was monitored at 414 nm (ϵ_{414} = 36 mM^{-1} cm^{-1}) (Childs & Bardsley, 1975).

Determination of Im Binding Constant (K_d). In a 400 μL volume, Im (5, 14, 23, 32, 41, 50, or 59 mM) was preincubated with 7 μM H170A hHRP in 20 mM Na_2HPO_4 at pH 6.0. The 300−550 nm difference spectra between Im-bound and Im-free H170A hHRP were obtained by subtracting the Im-free H170A hHRP spectrum from the spectra generated when Im-bound H170A hHRP was scanned against a reference cuvette containing the corresponding amount of Im in buffer.

Determination of the pH Profile for Guaiacol and ABTS Oxidation. The guaiacol and ABTS activities of native, wild-

Table 1: ABTS and H_2O_2 Concentrations Used in the Steady-State Kinetic Analysis

enzyme	[ABTS] (mM)	[H_2O_2] (mM)
native HRP	0.1−1.0	0.025−0.250
wild-type hHRP	0.1−1.0	0.025−0.250
H170 A hHRP	0.01−0.10	8.5−85.0
H170A hHRP + Im (25 mM)	0.2−2.0	0.025−0.250

type hHRP, and H170A hHRP were assayed at pH 4−10 at 20 °C. The 25 mM buffers used included HOAc/NaOAc (pH 4-5.5), NaH_2PO_4/Na_2HPO_4 (pH 6−8), and $HBO_3/Na_2B_4O_7$ (pH 8.5−10). NaCl (0.1 M) was added to maintain a constant ionic strength. A solution of guaiacol (5 mM) or ABTS (5 mM) and either native HRP (1 nM), wild-type hHRP (1 nM), or H170A hHRP (0.95 μM) was prepared in 1 mL of the appropriate buffer. In the case of H170A hHRP, similar incubations were carried out after preincubation for 2 h with 25 mM Im. H_2O_2 (0.5 mM) was added to initiate the reaction. Guaiacol consumption and ABTS cation radical production were monitored spectroscopically as described above.

Steady State Kinetics of ABTS Oxidation. The ABTS assay described above was used to determine the rate constants (eqs 1−3) for compound I formation (k_1) and substrate oxidation (k_2, k_3). ABTS oxidation was assayed using various concentrations of H_2O_2 and ABTS (Table 1). Native HRP (1 nM), wild-type hHRP (1 nM), H170A hHRP (191 nM), and H170A hHRP (95 nM plus 25 mM Im) were assayed at 25 °C. The HRP peroxidase cycle (eqs 1−3) is typically characterized by the following equation, a modified version of ping-pong kinetics where $v = -\mathrm{d[ABTS]}/\mathrm{d}t$:

$$2[\mathrm{HRP}]_o/v = [(k_2 + k_3)/k_2k_3](1/[\mathrm{ABTS}]) + (1/k_1)(1/[\mathrm{H_2O_2}]) \quad (4)$$

Normally, k_3 is 1−2 orders of magnitude smaller than k_2 so that eq 4 simplifies to eq 5.

$$2[\mathrm{HRP}]_o/v = (1/k_3)(1/[\mathrm{ABTS}]) + (1/k_1)(1/[\mathrm{H_2O_2}]) \quad (5)$$

A similar equation fits ABTS oxidation catalyzed by native HRP (Smith *et al.*, 1992). This equation includes k_u, a first-order rate constant that describes product release. Product release does not appear to limit the rate of guaiacol oxidation, so that a similar term is not required in eqs 4 and 5.

$$2[\mathrm{HRP}]_o/v = (1/k_3)(1/[\mathrm{ABTS}]) + (1/k_1)(1/[\mathrm{H_2O_2}]) + 1/k_u \quad (6)$$

Equation 6 was used to determine values for k_1, k_3, and k_u using measured velocities of ABTS radical cation production.

Resonance Raman Experiments. The 95 μM H170A hHRP sample (ferric form) in 20 mM phosphate buffer (pH 6.0) was examined directly after purification. Reduction to the ferrous state was accomplished by adding a slight excess of a freshly prepared solution of 60 mM $Na_2S_2O_4$ in 100 mM phosphate buffer (pH 6.0) to septum-sealed samples which were prepurged with argon gas for ∼10 min (monitored by UV−vis spectroscopy). Addition of appropriate amounts of 1 M H_3PO_4 to the above solutions changed their pH to 4.0.

Resonance Raman spectra were obtained on a custom spectrometer consisting of a McPherson (Acton, MA) Model 2061/207 single monochromator operated at a focal length of 0.67 m and a Princeton Instruments (Trenton, NJ) LN1100 CCD detector. Rayleigh scattering was attenuated by using Kaiser Optical (Ann Arbor, MI) notch filters. Excitation sources consisted of an Innova 302 krypton laser (413.1 and 350.7 nm) or a Liconix 4240NB He-Cd laser (441.6 nm). All laser lines were filtered through Applied Photophysics (Leatherhead, U.K.) optical glass or quartz prism monochromators to remove plasma emissions. Spectra were collected in a 90°-scattering geometry from solution samples contained in glass capillary tubes at room temperature. Spectral resolution was ∼5.5 cm^{-1}. CCl_4 was used as a standard for polarization. Indene and/or CCl_4 were used as the calibrants for the frequency shifts with the CCD spectrograph.

RESULTS

H170A hHRP Purification and Reconstitution. As described for the purification of earlier hHRP mutants (Newmyer & Ortiz de Montellano, 1995), nickel(II) nitrilotriacetic acid resin (NTA) (Qiagen) was used to purify H170A hHRP. This column purifies H170A hHRP to greater than 95% purity based on SDS−PAGE (not shown). Based on the Bradford assay, the yield of H170A hHRP is ∼20 mg/L of expression media, but spectroscopic analysis shows that the major form isolated (>90%) is the apoprotein. The heme content of the protein prior to Ni(II) NTA chromatography is not known, but at least some heme is stripped from the protein during this chromatographic step because heme slowly leaches from the column prior to protein elution. The purification of hHRP normally requires an additional Sepharose QFF (Pharmacia) column, but this column was not necessary with H170A hHRP because the protein from the Ni(II) NTA column was of sufficient purity. The mutant was reconstituted with 1 equiv of hemin in Na_2HPO_4 buffer at pH 4 to prevent binding of heme to the polyhistidine tag. After 30 min, the protein was brought to pH 6.0. The bound heme was judged to be specifically bound to the heme pocket based on its spectroscopic properties and the finding that the Soret absorbance of the reconstituted protein did not decrease when the protein was passed through BSA-bound Sepharose, which binds and removes nonspecifically bound heme. After this reconstitution protocol, ∼80% of the H170A hHRP was present as the holoenzyme. Nonspecific binding of a fraction of the heme, followed by its removal by the BSA column, rationalizes the lower than 100% efficiency of reconstitution. The concentration of H170A hHRP in all the experiments reported here refers to the holoenzyme fraction.

Spectroscopic Characterization. The spectrum of H170A hHRP differs markedly from that of wild-type hHRP and is sensitive to pH (Figure 1, Table 2). At pH 5, 6, and 7, the Soret band of H170A hHRP appears at λ_{max} = 412, 414, and 414 nm, respectively. This absorption maximum is red-shifted 9−11 nm from that of hHRP in the same pH range. The visible region of the spectrum, which displays significant α/β bands at pH 5−7, is also altered. These changes suggest that a significant portion of the heme in H170A hHRP is coordinated to two strong axial ligands. At pH 4, the α/β bands in the spectrum of H170A hHRP diminish, and charge transfer bands appear. The resemblance of the visible region of the spectrum of the mutant at pH 4 to that of wild-type hHRP suggests that at pH 4 the mutant is predominantly high-spin. The Soret (λ_{max} = 370 nm) is also blue-shifted from that of the spectrum at neutral pH.

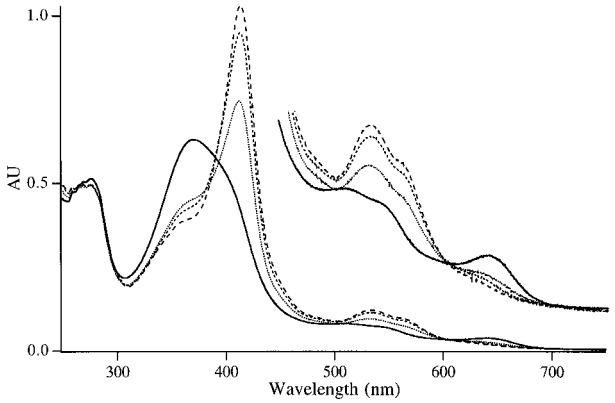

FIGURE 1: Spectra of H170A hHRP at pH 4 (—), pH 5 (···), pH 6 (---), and pH 7 (— —).

Table 2: Spectroscopic Properties of H170A hHRP and Wild-Type hHRP at Different pH Values[a]

protein	pH	Soret (nm)	α/β (nm)	CT1/CT2[b] (nm)
wild-type hHRP	4	406		503/641
	5	403		503/641
	6	403		503/641
	7	403		503/641
H170A hHRP	4	370 (399 sh)		512 (545 sh)/641
	5	412	564 (sh)/532	641
	6	414	564 (sh)/533	
	7	414	563 (sh)/534	

[a] sh = shoulder. [b] CT, charge transfer band.

Resonance Raman Spectroscopy. The rRaman spectrum of H170A hHRP, like the UV−visible spectrum, is different from that of the wild-type enzyme (Terner & Reed, 1984) and is pH-dependent. Figure 2 shows the rRaman spectra of ferric H170A hHRP at pH 6.0 and pH 4.0. In the pH 6.0 spectrum, we observe a polarized band at 1505 cm^{-1} (ν_3) and a depolarized band at 1641 cm^{-1} (ν_{10}) which are characteristic of a 6cLS heme (Evangelista-Kirkup et al., 1985). Other observed rRaman frequencies such as 1579 cm^{-1} (ν_2) and 1583 cm^{-1} (ν_{19}) also suggest that the predominant species at pH 6.0 is a 6cLS heme (Evangelista-Kirkup et al., 1985). At pH 4.0, the Soret absorption in the UV−vis spectrum of H170A hHRP becomes broad, and its maximum is blue-shifted to 370 nm. We have obtained rRaman spectra of this form of the enzyme with 413.1- and 350.7-nm excitation wavelengths that bracket the Soret maximum (Figure 2). Both of these spectra are characteristic of a 5cHS heme species. In the 413.1-nm spectrum, strong bands at 1492 cm^{-1} (ν_3) and 1571 cm^{-1} (ν_2) arise from a ferric 5cHS heme (Asher & Schuster, 1979; Evangelista-Kirkup et al., 1985; Smulevich et al., 1988; Palaniappan & Terner, 1989; Adachi et al., 1993). The band at 1628 cm^{-1} in this spectrum probably belongs to a vinyl mode. The rRaman spectra obtained with near-UV excitation are usually dominated by porphyrin skeletal modes ν_2 and ν_{10} (Palaniappan & Terner, 1989). The frequencies of these two modes in the 350.7-nm rRaman spectrum of the pH 4.0 form are at 1573 and 1628 cm^{-1}, respectively. A weaker ν_3 band is also seen at 1492 cm^{-1}. All these frequencies are typical of a ferric 5cHS heme. Because of the broad nature of the Soret absorption at pH 4.0, we have searched for species other than a 5cHS heme with Q-band excitation (514.5 nm, data not shown) but have found none. The present rRaman data reveal that the predominant ferric H170A hHRP species

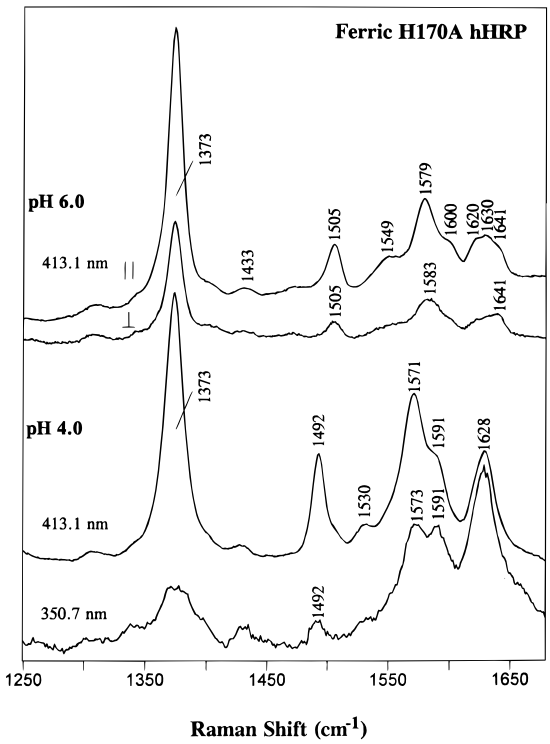

FIGURE 2: Resonance Raman spectra of ferric H170A hHRP at pH 6.0 (upper two traces) and pH 4.0 (lower two traces). The pH 6 spectra were obtained with 413.1-nm excitation in parallel and perpendicular polarization. The pH 4 spectra were obtained with 413.1- and 350.7-nm excitation. The incident laser power in all cases was ~10 mW.

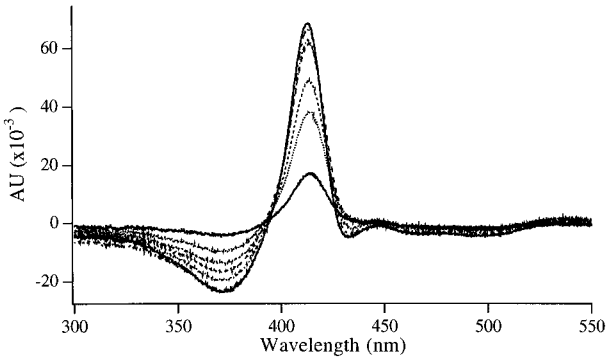

FIGURE 3: Difference spectra for Im-bound versus Im-free H170A hHRP at pH 6.0. The Im concentrations were 5, 14, 23, 32, 41, 50, and 59 mM.

at pH 6.0 and pH 4.0 are a 6cLS heme and a 5cHS heme, respectively.

Im Binding Constant. Addition of Im causes minor changes in the spectrum of H170A hHRP. Increasing the Im concentration from 5 to 59 mM at pH 6.0 produces the difference spectra shown in Figure 3. The addition of Im sharpens the Soret band with $\lambda_{max} = 414$ nm. The changes in absorption between 372 and 414 nm, and the corresponding Im concentrations, were fit to the equation:

$$\frac{\Delta A}{\Delta A_{max}} = \frac{[S]}{K_d + S} \quad (7)$$

The K_d value calculated from this equation is 22 ± 4 mM. Addition of Im to wild-type HRP causes no detectable change in the absorption maxima even at very high concentrations.

Im Rescue of Guaiacol and ABTS Activities. H170A hHRP has optimal activity when stored at pH 6.0, but this

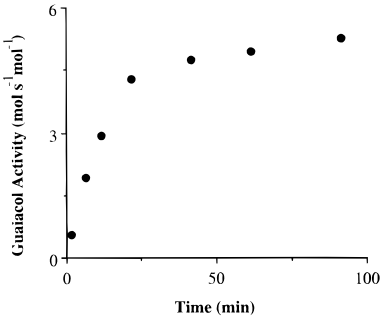

FIGURE 4: Rescue of H170A hHRP guaiacol oxidizing activity as a function of the time of preincubation with 16 mM Im at pH 7. The assay solution contained 0.5 μM H170A hHRP in 20 mM Na_2HPO_4 (pH 7.0): 0.5 mM H_2O_2 was added to initiate the reaction.

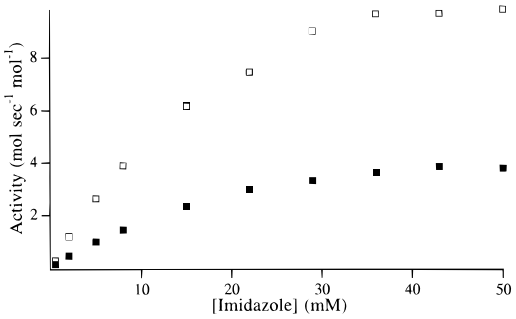

FIGURE 5: Influence of Im (0.5−50 mM) on the H170A hHRP-catalyzed oxidation of ABTS (at pH 5.0) and guaiacol (at pH 6.0): guaiacol (■), ABTS (□).

activity is significantly lower than that of wild-type hHRP at the same pH. H170A hHRP displays 0.003% of the guaiacol and 0.004% of the ABTS peroxidase activity of wild-type hHRP. However, the catalytic activity of H170A hHRP can be partially rescued by exogenous Im. If H170A hHRP is preincubated with Im at pH 6.0 and aliquots are taken to measure the peroxidase activity as a function of time, the activity is found to increase with time and to level off after ~40 min (Figure 4). Dilution of the Im-preincubated enzyme into assay buffer containing the same Im concentration as the parent solution gave the same activity as that measured when the assay buffer did not contain Im. The off-rate for Im dissociation thus appears to be slow relative to the time scale of the activity assay. Im was therefore preincubated with the H170A mutant for 2 h prior to the peroxidase activity assay, and the assay was carried out in buffer that did not contain Im. An advantage of this protocol is that the high Im concentrations required for binding to H170A hHRP are diluted in the assay mixture and therefore are less likely to interfere with activity measurements (Kuo & Fridovich, 1988).

The activity of H170A hHRP is increased in a saturable manner by Im, in accord with the finding that the spectroscopic changes caused by Im are also saturable. The concentration dependence of both the guaiacol and ABTS activities on Im is the same, as expected if exogenous Im facilitates catalytic steps other than electron abstraction from the substrate. When the data in Figure 5 are fit to eq 8, the K_m values for Im are calculated to be 24 mM for the enhancement of both guaiacol and ABTS peroxidation.

$$\frac{r}{V_{max}} = \frac{[S]}{K_m + [S]} \qquad (8)$$

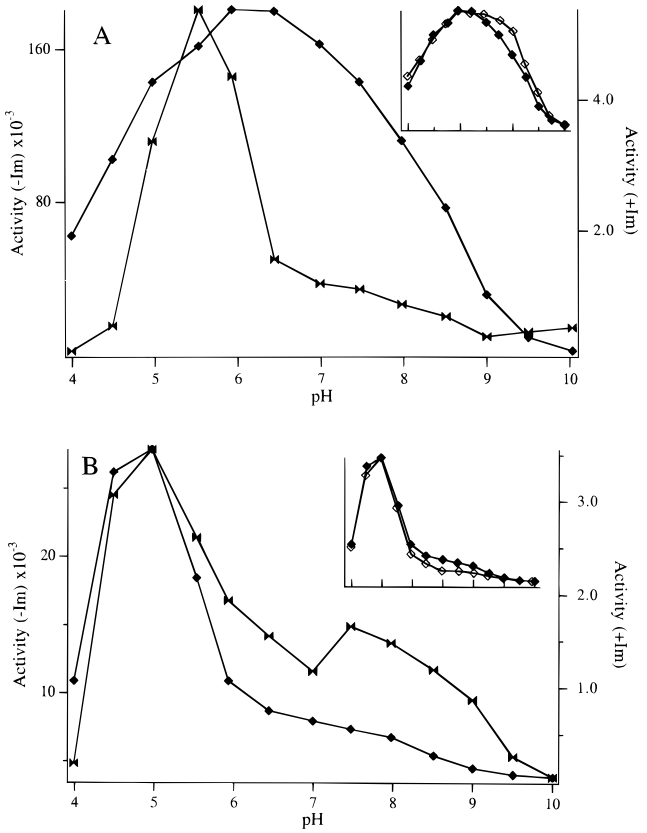

FIGURE 6: pH profiles of the guaiacol (A) and ABTS (B) activities as catalyzed by H170A HRP in the absence and presence of Im. The inset shows a comparison of the activity of H170A hHRP in the presence of 25 mM Im with wild-type hHRP. Wild-type hHRP activity is scaled down to match that of Im-rescued H170A hHRP: based on activities measured at their respective pH optima, WT hHRP guaiacol activity is 320-fold greater and ABTS activity 280-fold greater than the activity of Im-rescued H170A hHRP: H170A hHRP (solid bow ties); H170A hHRP + 25 mM Im (♦); wild-type hHRP (◊). The units of activity are mol s^{-1} mol^{-1}.

The identity of these K_m values and the K_d obtained by spectroscopic measurements argues that the enhancement in activity involves binding of Im to the protein. The calculated V_{max} values indicate that, in the presence of Im, H170A hHRP has 0.8% of the guaiacol activity and 0.5% of the ABTS activity of wild-type hHRP. Saturating Im concentrations thus improve the guaiacol activity 260-fold and the ABTS activity 125-fold relative to the activity of H170A hHRP without Im.

pH Profile of H170A hHRP. H170A hHRP exhibits a different pH profile than wild-type hHRP for the oxidation of guaiacol, but addition of 25 mM Im to H170A hHRP gives rise to a pH profile that closely resembles that of the wild-type protein (Figure 6A). The pH profiles for the oxidation of ABTS by H170A hHRP and wild-type hHRP are not very different, although the decline of the activity at pH values above 6 is more gradual for the mutant than the native protein (Figure 6B). This small difference in activity at higher pH is virtually eliminated by addition of 25 mM Im to the H170A mutant. Depending on the substrate, the pH profile of native HRP is governed at low pH by reduction of either compound I or compound II, but at neutral to high pH is generally controlled by reduction of compound II (Marnett et al., 1986). In either case, the ionization state of the distal histidine is a major determinant of the pH profile. The alterations in the pH-dependence of guaiacol and ABTS

Table 3: Kinetic Rate Constants for H170A hHRP Deduced from a Steady-State Kinetic Analysis of the Oxidation of ABTS[a]

enzyme	k_1 ($M^{-1}s^{-1}$)	k_3 ($M^{-1}s^{-1}$)	k_u (s^{-1})
native HRP	$4.7\ (\pm 0.0) \times 10^6$	$7.2\ (\pm 0.4) \times 10^5$	$3.4\ (\pm 0.0) \times 10^2$
wild-type hHRP	$4.4\ (\pm 0.2) \times 10^6$	$8.2\ (\pm 0.1) \times 10^5$	$4.1\ (\pm 1.1) \times 10^2$
H170A hHRP	$1.6\ (\pm 1.2) \times 10^1$	$3.0\ (\pm 3.4) \times 10^4$	$4.4\ (\pm 0.4) \times 10^{-1}$
H170A hHRP + Im	$2.4\ (\pm 0.9) \times 10^4$	$4.8\ (\pm 1.4) \times 10^3$	$1.6\ (\pm 0.5) \times 10^0$

[a] Each protein was analyzed twice, and the reported error shows the variation between the two values.

oxidation caused by the H170A mutation suggest that the proximal histidine ligand also influences the pH profile. The proximal histidine ligand may modulate the pH dependence of the reduction of compound II, or may help to determine whether compound II is the rate-determining step of the reaction. The finding that addition of Im to H170A hHRP restores the wild-type pH profiles for oxidation of both substrates suggests that the protein environment surrounding the heme is not greatly altered by removal of the heme tether.

Steady State Kinetics with ABTS as the Substrate. Compound I of HRP is obtained by adding 1 equiv of H_2O_2 and compound II by subsequently adding 1 equiv of ferrocyanide. Addition of a second equivalent of ferrocyanide regenerates the resting ferric state. Compound I and compound II could not be generated in a spectroscopically detectable manner when H170A hHRP was thus treated whether Im was present or not. Addition of excess (100 equiv) H_2O_2 causes the Soret absorption to decrease, as normally observed for compound I, but this decrease in absorbance continues until there is no further Soret absorbance, a clear indication that the heme group had been destroyed. Addition of ferrocyanide during this process does not lead to recovery of the Soret absorbance but prevents its further decay. Nevertheless, the formation of transient compound I and II intermediates, or of species with similar oxidative properties, is required to rationalize the catalytic activity of H170A hHRP in the absence and presence of Im.

To obtain rate constants for the formation of compound I or its equivalent, a steady-state kinetic analysis was carried out with native HRP, wild-type hHRP, and H170A hHRP. According to eq 6, the reciprocal of a range of measured velocities can be linearly related to the reciprocal of the ABTS concentration. Varying the H_2O_2 concentration yields a series of roughly parallel lines (not shown). The reciprocals of the slopes of this series of lines were averaged to obtain k_3. The primary intercepts were plotted versus the reciprocal of the H_2O_2 concentration. The reciprocal of the slope of this secondary plot gave k_1, the rate constant of the reaction of H170A hHRP with H_2O_2 to give a compound I-like intermediate. The reciprocal of the secondary intercept gives k_u, the product release constant. The resulting values are shown in Table 3. The high error reported for H170A hHRP stems from the need to assay small ABTS concentrations because this mutant is very sensitive to inhibition by higher ABTS concentrations. Inhibition by elevated ABTS concentrations has been reported (Childs & Bardsley, 1975). The most striking change in the kinetic constants is the decrease in k_1 for H170A hHRP, which is 5 orders of magnitude lower than that for native HRP or wild-type hHRP (Table 3). In the presence of 25 mM Im, which saturates half of the available enzyme active sites ($K_d = 22$ mM), compound I formation is partially rescued, as indicated by the 1500-fold

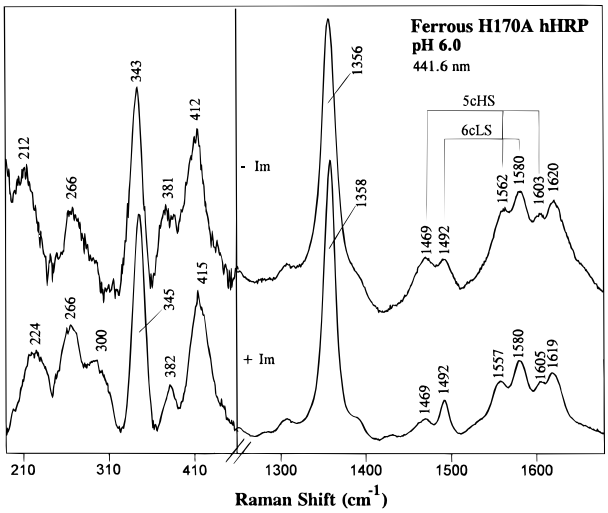

FIGURE 7: Resonance Raman spectra of ferrous H170A hHRP at pH 6.0 using 441.6-nm excitation, ~10 mW. The sample for the upper trace contained no exogenous Im. The sample for the lower spectrum contained a 250-fold excess of Im (24 mM).

increase in the value of k_1. The constant k_3 normally represents the rate of reduction of compound II by electron transfer from the substrate, but this interpretation may not be correct here because it assumes that reduction of compound II is the rate-limiting step in catalytic turnover (i.e., $k_3 \ll k_2$). In view of the failure to spectroscopically detect either compound I or compound II, the rate-limiting step in the overall catalytic process is unclear. Nevertheless, whether the value identified as k_3 is actually k_3, k_2, or $(k_2 + k_3)/k_2k_3$, it is clear that substrate turnover is only modestly affected by removal of the proximal ligand. Addition of Im does not rescue, and appears to actually inhibit, ABTS oxidation by H170A hHRP (Table 3). The reason for the inhibitory effect of Im is not known, but one possible explanation is that it is oxidized in competition with ABTS. The differences in k_u suggest that product dissociation is slower for H170A hHRP in both the absence and presence of Im than it is for the wild-type protein.

DISCUSSION

Replacement of the proximal histidine ligand by an alanine yields an hHRP mutant that is spectroscopically distinct from wild-type hHRP at pH 5−7 (Table 2). In this pH range, the spectrum of the H170A mutant is characterized by a sharp Soret maximum at ~414 nm and α/β bands at ~563 and ~534 nm (Figure 1), in contrast to the spectrum of the wild-type protein which has a Soret maximum at 403 nm and no α/β bands (Table 2). These spectroscopic differences, particularly the presence of α/β bands, suggest that the iron in H170A hHRP is coordinated to two strong axial ligands rather than the single His ligand present in the wild-type protein. This conclusion is supported by resonance Raman studies, which show that the ferric H170A mutant is predominantly a hexacoordinate, low-spin species. It is puzzling that ferric H170A hHRP contains a 6cLS heme center at neutral pH because the proximal histidine ligand has been eliminated. We have studied the rRaman spectrum of ferrous H170A hHRP at pH 6.0 to further delineate the nature of the coordinating ligands (Figure 7). The rRaman bands in the high-frequency region are a mixture of porphyrin skeletal modes from a 5cHS heme and a 6cLS heme. The

dominant band at 1356 cm^{-1} (ν_4) is as expected for ferrous hemes. Other strong bands at 1469 cm^{-1} (ν_3), 1562 cm^{-1} (ν_2), and 1603 cm^{-1} (ν_{10}) are indicative of a 5cHS heme (Sun *et al.,* 1993). A second set of bands at 1492 cm^{-1} (ν_3) and 1580 cm^{-1} (ν_2) reveals the coexistence of a 6cLS heme species (Sun *et al.,* 1996). In the low-frequency region, we observe a band at 212 cm^{-1} that we assign to a ν(Fe−His) mode of the 5cHS ferrous species. Previous studies have shown that the ν(Fe−His) mode is strongly enhanced with 441.6-nm excitation for 5cHS ferrous hemes with a proximal histidine ligand and lies in the range of ∼210−250 cm^{-1} (Kincaid *et al.,* 1979; Kitagawa *et al.,* 1979; Teraoka & Kitagawa, 1981; Choi & Spiro, 1983; Bangcharoenpaurpong *et al.,* 1984; Smulevich *et al.,* 1988; Sun *et al.,* 1993). The relative intensity of the 212 cm^{-1} band observed in Figure 7 is not as high as that of the ν(Fe−His) band in compounds such as ferrous myoglobin, HRP, and CCP. This is understandable because ferrous H170A hHRP is a mixture of 5cHS and 6cLS hemes, both of which contribute to the intensities of other rRaman bands. The coordinating histidine in H170A hHRP is most probably the distal histidine located directly above the heme plane in the wild-type enzyme. In the ferrous state, binding to an as yet unknown axial ligand (possibly water) leads to the equilibrium between 5cHS and 6cLS species. In the ferric state, the second axial ligand (aqua/hydroxo) binds more strongly since the H170A hHRP is observed to have primarily a 6cLS heme.

Lowering the pH to 4.0 greatly alters the H170A UV−vis and rRaman spectra. The iron coordination state clearly undergoes a major change between pH 4 and 5 (Figure 1, Table 2). The UV−vis and rRaman spectra of the H170A mutant at pH 4.0 are similar to those of the H175G mutant of CCP at pH 7.0. Although the crystal structure of the H175G CCP mutant shows that the heme iron is coordinated to two water molecules (McRee *et al.,* 1994), solution rRaman data suggest that the heme iron is 5cHS, and, hence, only coordinated to one axial ligand (J. Sun, M. Fitzgerald, D. Goodin, and T. M. Loehr, unpublished data). It is very likely that H170A hHRP at pH 4.0 has a similar 5cHS structure.

The spectroscopic changes observed at pH 7 on binding of Im to the H170A hHRP and H175G CCP mutants differ significantly. Binding of Im to the bisaquo H175G CCP mutant at this pH sharpens the broad Soret absorption of the mutant and shifts it from 395 to 408 nm without the detectable appearance of α,β-bands (McRee *et al.,* 1994). The crystal structure of the H175G CCP−Im complex shows that the proximal water ligand is replaced by an Im (McRee *et al.,* 1994), accounting for the observed spectroscopic changes. In contrast, the binding of Im to H170A hHRP at pH 7 causes a sharpening of the Soret band without a shift in its position. The minor changes observed on binding of Im to H170A hHRP support the conclusion that the iron in the mutant is coordinated not to two water molecules but to the distal histidine and a water. When Im is present, the 6cLS population is increased for ferrous H170A hHRP, as judged by the relative rRaman intensity of the 1492 vs 1469 cm^{-1} band (Figure 7). This increase could be caused by formation of $His_{distal}-Fe^{II}-Im$ or $Im-Fe^{II}-Im$, in addition to the original $His_{distal}-Fe^{II}-X$ (X = water or ?) 6cLS species. But, there is also a new 5cHS ferrous heme species of H170A hHRP. This is indicated by a new band at 224 cm^{-1} in the low-frequency region that we assign to ν(Fe−Im) (Figure 7). When adjusted for the mass of the extra -CH_2- group of histidine, the observed 224 cm^{-1} frequency is lowered to ∼210 cm^{-1}. This value is markedly lower than the ∼245 cm^{-1} Fe−His stretching frequency measured for the wild-type enzyme that is indicative of strong hydrogen bonding of the proximal ligand (Teraoka & Kitagawa, 1981). The very low Fe−Im frequency in the H170A hHRP/Im complex indicates that such a hydrogen bonding interaction in not reestablished. The binding of Im to H170A hHRP at pH 6.0 (K_d = 22 mM) is ∼10-fold weaker than the binding of Im to H175G CCP at pH 7.0 (K_d = 2.7 mM) (McRee *et al.,* 1994). A part of the difference in the binding of Im by H170A hHRP and H175G CCP may be due to the different concentrations of protonated (ImH^+) and unprotonated Im at the pH values used for the measurements.

In the absence of a substrate, the reaction of H170A hHRP with H_2O_2 does not give spectroscopically detectable compound I or compound II species. The immediate decrease in the Soret band absorbance observed with excess H_2O_2 is not due to the formation of a normal compound I intermediate because the absorbance loss is not reversed by the addition of ferrocyanide. Furthermore, the loss of Soret absorbance continues with time until the chromophore is no longer present. The same observation is made in the presence or absence of exogenous Im. The H170A hHRP mutant differs in this regard from the H175G CCP mutant, which gives a compound II-like spectrum in the absence or presence of Im (McRee *et al.,* 1994). The failure to observe a ferryl species with H170A hHRP is puzzling in view of its formation with H175G CCP. A likely explanation for the finding that H170A hHRP does not react with H_2O_2 to give a detectable ferryl spectrum is that the distal histidine is coordinated to the iron atom in most of the enzyme (see below). The observed catalytic activity may be due to a small fraction of the protein in which the iron is not coordinated to the distal histidine, in which case the spectroscopic changes may not be sufficient to afford a detectable compound I or compound II spectrum.

The peroxidase activity of H170A hHRP is lower than that of the wild-type enzyme, but the activity of the mutant is partially rescued in a saturable manner by Im. The rate constant k_1 for compound I formation is lower for the mutant than wild-type enzyme by a factor of 2.75×10^5 (Table 3). Addition of Im (25 mM) to H170A hHRP produces an impressive 1500-fold improvement in the rate of compound I formation, although the rate is still ∼180-fold lower than that for wild-type hHRP (Table 3). The proximal His-170 iron ligand may facilitate compound I formation by (a) providing a heme tether that pulls the iron out of the heme plane, promoting the pentacoordinate ligation state required for reaction of the iron with the peroxide, and/or (b) donating electron density to the heme iron to facilitate peroxide O−O bond cleavage. The spectroscopic evidence that the iron in H170A hHRP is hexacoordinate low-spin in both the absence and presence of exogenous Im indicates that Im, unlike the normal histidine ligand, does not effectively impose a pentacoordinated state on the iron atom. This suggests that the rate of compound I formation will be reduced in the mutant in the presence of exogenous Im regardless of whether the distal ligand is the distal histidine or a water molecule. A precedent for this is provided by metmyoglobin, in which the sixth iron ligand is a water molecule with a stabilizing hydrogen bond to a distal histidine. The rate of

the reaction of metmyoglobin with H_2O_2 at pH 8.5 (23 °C) to give a ferryl species is 1.4×10^2 M^{-1} s^{-1} (Fox *et al.*, 1974; Yonetani & Schleyer, 1967). Modification of the distal histidine with cyanogen bromide to give a protein in which the iron is penta- rather than hexacoordinated (i.e., has no distal water ligand) improves the rate of ferryl complex formation to 5.2×10^7 M^{-1} s^{-1} (Morishima *et al.*, 1989; Modi *et al.*, 1991), a value higher than that for native HRP (Table 3).

The binding of exogenous Im may stimulate the activity of H170A hHRP by providing increased electron density for cleavage of the peroxide O−O bond or, as a consequence of its ability to donate electrons, by promoting dissociation of the distal histidine from the iron. Conversely, the failure of exogenous Im to fully rescue the catalytic activity of H170A hHRP may reflect its inability to maintain the bulk of the iron in a pentacoordinated state. The importance for the iron coordination state of tethering it to a tightly constrained proximal histidine ligand is evident in extended X-ray absorption (EXAFS) studies of HRP and myoglobin in which the heme peripheral substituents were varied (He *et al.*, 1996). These studies show that the changes in axial ligand bond lengths caused by the alterations in heme substituents are exerted in HRP exclusively on the distal side, presumably because the proximal histidine is rigidly held by hydrogen bonds, whereas the bonds to both the proximal and distal ligands are affected in myoglobin, a protein in which the proximal histidine is not so constrained. A major function of the proximal histidine ligand in HRP is therefore to tether the heme iron to maintain it in a pentacoordinated state and to prevent its coordination to the distal histidine. The strongly hydrogen-bonded proximal histidine may also contribute to rupture of the O−O bond in the formation of compound I.

REFERENCES

Adachi, S., Nagano, S., Ishimori, K., Watanabe, Y., Morishima, I., Egawa, T., Kitagawa, T., & Makino, R. (1993) *Biochemistry 32*, 241−252.

Asher, S. A., & Schuster, T. M. (1979) *Biochemistry 18*, 5377−5387.

Banci, L., Bertini, I., Turano, P., Tien, M., & Kirk, T. K. (1991) *Proc. Natl. Acad. Sci. U.S.A. 88*, 6956−6960.

Bangcharoenpaurpong, O., Schomacker, K. T., & Champion, P. (1984) *J. Am. Chem. Soc. 106*, 5688−5698.

Barrick, D. (1994) *Biochemistry 33*, 6546−6554.

Barrick, D. (1995) *Curr. Opin. Biotechnol. 6*, 411−418.

Childs, R. E., & Bardsley, W. G. (1975) *Biochem. J. 145*, 93−103.

Choi, S., & Spiro, T. G. (1983) *J. Am. Chem. Soc. 105*, 3683−3692.

Choudhury, K., Sundaramoorthy, M., Hickman, A., Yonetani, T., Woehl, E., Dunn, M. F., & Poulos, T. L. (1994) *J. Biol. Chem. 269*, 20239−20249.

Dawson, J. H. (1988) *Science 240*, 433−439.

den Blaauwen, T., & Canters, G. W. (1993) *J. Am. Chem. Soc. 115*, 1121−1129.

DePillis, G. D., Decatur, S. M., Barrick, D., & Boxer, S. G. (1994) *J. Am. Chem. Soc. 116*, 6981−6982.

Doeff, M. M., & Sweigert, D. A. (1982) *Inorg. Chem. 21*, 3699.

Du, P., & Loew, G. H. (1995) *Biophys. J. 68*, 69−80.

Evangelista-Kirkup, R., Crisanti, M., Poulos, T. L., & Spiro, T. G. (1985) *FEBS Lett. 190*, 221−226.

Finzel, B. C., Poulos, T. L., & Kraut, J. (1984) *J. Biol. Chem. 259*, 13027−13036.

Fox, J. B., Nicholas, R. A., Ackerman, S. A., & Swift, C. E. (1974) *Biochemistry 13*, 5178−5186.

Furhop, J. H., & Smith, K. M. (1975) *Laboratory Methods* (Smith, K. M., Ed.) in *Porphyrins and Metalloporphyrins*, pp 757−869, Elsevier, Amsterdam.

Goodin, D. B., & McRee, D. E. (1993) *Biochemistry 32*, 3313−3324.

He, B., Sinclair, R., Copeland, B. R., Makino, R., Powers, L. S., & Yamazaki, I. (1996) *Biochemistry 35*, 2413−2420.

Kincaid, J., Stein, P., & Spiro, T. G. (1979) *Proc. Natl. Acad. Sci. U.S.A. 76*, 549−552; 4156 (errata).

Kitagawa, T., Nagai, K., & Tsubaki, M. (1979) *FEBS Lett. 104*, 376−378.

Kunishima, N., Fukuyama, K., Matsubara, H., Hatanaka, H., Shibano, Y., & Amachi, T. (1994) *J. Mol. Biol. 235*, 331−344.

Kuo, C., & Fridovich, I. (1988) *J. Biol. Chem. 263*, 3811−3817.

Marnett, L. J., Weller, P., & Battista, J. R. (1986) in *Cytochrome P450: Structure, Mechanism, and Biochemistry* (Ortiz de Montellano, P. R., Ed.) pp 29−76, Plenum Press, New York.

McRee, D. E., Jensen, G. M., Fitzgerald, M. M., Siegel, H. A., & Goodin, D. B. (1994) *Proc. Natl. Acad. Sci. U.S.A. 91*, 12847−12851.

Modi, S., Behere, D. V., Mitra, S., & Bendall, D. S. (1991) *J. Chem. Soc., Chem. Commun.*, 830−831.

Moore, G. R., & Williams, R. J. P., (1977) *FEBS Lett. 79*, 229−232.

Moore, G. R., Pettigrew, G. W., & Rogers, N. K. (1986) *Proc. Natl. Acad. Sci. U.S.A. 83*, 4998−4999.

Morishima, I., Shiro, Y., Adachi, S., Yano, Y., & Orii, Y. (1989) *Biochemistry 28*, 7582−7586.

Newmyer, S. L., & Ortiz de Montellano, P. R. (1995) *J. Biol. Chem. 270*, 19430−19438.

Ortiz de Montellano, P. R. (1992) *Annu. Rev. Pharmacol. Toxicol. 32*, 89−107.

Palaniappan, V., & Terner, J. (1989) *J. Biol. Chem. 264*, 16046−16053.

Patterson, W. R., & Poulos, T. L. (1995) *Biochemistry 34*, 4331−4341.

Poulos, T. L., Edwards, S. L., Wariishi, H., & Gold, M. H. (1993) *J. Biol. Chem. 268*, 4429−4440.

Smith, A. T., Sanders, S. A., Thorneley, R. N. F., Burke, J. F., & Bray, R. C. (1992) *Eur. J. Biochem. 207*, 507−519.

Smulevich, G., Mauro, J. M., Fishel, L. A., English, A. M., Kraut, J., & Spiro, T. G. (1988) *Biochemistry 27*, 5477−5485.

Smulevich, G., Neri, F., Willemsen, O., Choudhury, K., Marzocchi, M. P., & Poulos, T. L. (1995) *Biochemistry 34*, 13485−13490.

Sun, J., Wilks, A., Ortiz de Montellano, P. R., & Loehr, T. M. (1993) *Biochemistry 32*, 14151−14157.

Sun, J., Kahlow, M. A., Kaysser, T. M., Osborne, J. P., Hill, J. J., Rohlfs, R. J., Hille, R., Gennis, R. B., & Loehr, T. M. (1996) *Biochemistry 35*, 2403−2412.

Teraoka, J., & Kitagawa, T. (1981) *J. Biol. Chem. 256*, 3969−3977.

Terner, J., & Reed, D. E. (1984) *Biochim. Biophys. Acta 789*, 80−86.

Tondreau, G. A., & Sweigert, D. A. (1984) *Inorg. Chem. 23*, 1060.

Traylor, T. G., & Popovitz-Biro, R. (1988) *J. Am. Chem. Soc. 110*, 239−243.

Walker, F. A., Lo, M. W., & Ree, M. T. (1976) *J. Am. Chem. Soc. 98*, 5552.

Yonetani, T., & Schleyer, H. (1967) *J. Biol. Chem. 242*, 1974−1979.

Zeng, J., & Fenna, R. E. (1992) *J. Mol. Biol. 226*, 185−207.

BI9609331